Pressure-induced structural phase transition in bulk $Zn_{0.98}Mn_{0.02}O$ by angular dispersive X-ray diffraction

CrossMark

Chih-Ming Lin [a],*, Kung-Liang Lin [b], Yu-Ker Chern [c], Chia-Hung Hsu [a], Hwo-Shuenn Sheu [d], Yen-Fa Liao [d], Yuen-Wuu Suen [c], Sheng-Rui Jian [e],*, Jenh-Yih Juang [f],*

[a] Department of Applied Science, National Hsinchu University of Education, Hsinchu 30014, Taiwan
[b] Industrial Technology Research Institute, Hsinchu 30014, Taiwan
[c] Department of Physics, National Chung Hsing University, Taichung 402, Taiwan
[d] National Synchrotron Radiation Research Center, 101 Hsin-Ann Road, Hsinchu Science Park, Hsinchu 30076, Taiwan
[e] Department of Materials Science and Engineering, I-Shou University, Kaohsiung 840, Taiwan
[f] Department of Electrophysics, National Chiao Tung University, Hsinchu 300, Taiwan

ARTICLE INFO

ABSTRACT

The high pressure induced phase transition in bulk $Zn_{0.98}Mn_{0.02}O$ at ambient temperature have been investigated using angular-dispersive X-ray diffraction (ADXRD) under high pressure up to around 13.80 GPa. For loading run, *in situ* ADXRD measurements found that a würtzite-to-rocksalt structural phase transition pressure of bulk $Zn_{0.98}Mn_{0.02}O$ began at 7.35 GPa. The fitting of volume compression data to the third-order Birch–Murnaghan equation of state yielded that the zero-pressure isothermal bulk moduli and the first-pressure derivatives were 157(8) GPa and 8(3) for the B4 phase, respectively. When decompress bulk $Zn_{0.98}Mn_{0.02}O$ to ambient pressure a large part of the bulk $Zn_{0.98}Mn_{0.02}O$ reverted to the B4 phase and only a small amount of the metastable B1 phase remained. We have exhibits the pressure dependence of lattice constant a and c axis, and the normalized ratio c/a of the bulk $Zn_{0.98}Mn_{0.02}O$. Possible pressure-induced phase transition mechanisms were explored by examining the cell parameters and the internal structural parameter (u) with pressures. The effect of the $3d$ electrons of manganese to increase the nearest-neighbor distance of O to Zn (Mn) parallel to the c axis may be the main reason for the phase transition of bulk $Zn_{0.98}Mn_{0.02}O$. An increase in the u value with pressure indicates that the B4-to-B1 phase transformation in bulk $Zn_{0.98}Mn_{0.02}O$ is likely via the hexagonal path.

© 2014 Elsevier B.V. All rights reserved.

1. Introduction

Zinc oxide (ZnO) based ternary compound semiconductors have been attracting extensive research interest over the last decade due to their versatile applications in opto-electronic devices as well as in magnetically active quantum semiconductor structures associated with spintronics. For instance, non-magnetic ions doped ZnO, such as $Zn_{1-x}Mg_xO$ and $Zn_{1-x}Cd_xO$, has been demonstrated to be capable of tuning both the band gap and the lattice constant which might be significant for opto-electronic applications [1]. On the other hand, the diluted magnetic semiconductors (DMSs) made of $Zn_{1-x}TM_xO$ (TM = transition metals) exhibiting room-temperature ferromagnetism (RTFM) undoubtedly will play very important role in the studies of basic physical properties such as the spin transport and dynamics [2–6]. Among the entire family

of transition metals (Sc → Cu), manganese-doping has received most attention owing to its matched crystal ionic radii with Zn^{2+} (Mn^{2+} = 0.91 Å and Zn^{2+} = 0.83 Å)[7] and large magnetic moment ($S = 5/2$, $L = 0$). However, depending on the detailed process conditions, substantial discrepancies in the observed RTFM exist in various $Zn_{1-x}Mn_xO$ systems (x = 0.01–0.08) [7–11]. As a result, detailed investigation on the effect of the $3d$ electrons of manganese to the Zn–O bonding, especially the nearest-neighbor distance of O to Zn (Mn), is important as it may shed some light for resolving the discrepancies.

Pioneering experimental works carried out by Bates et al. [12] proposed that bulk ZnO went through a structural phase transition from würtzite (B4) to rocksalt (B1) phase under high pressure at ambient temperature. Recently, it has been well-established that the pressure at which the B4-to-B1 phase transition takes place is around 8.7–10.0 GPa with a volume change ($\Delta V/V$) of 16.7–18.13% [12–17]. Table 1 summaries the starting and completing pressures of the B4-to-B1 phase transition for bulk ZnO probed by various methods. These results are in line with predictions

---

Table 1
The starting and completing pressures of the würtzite to rocksalt phase transition and the probing methods of bulk ZnO under high pressure.

Starting pressure (GPa)	Completing pressure (GPa)	Two phases coexist pressure range (GPa)	Method[a]
9.5			XRD [12]
9.0	9.6	0.6	EDXRD [15]
10.0	15.0	5.0	EDXRD [16]
9.1	9.6	0.5	EDXRD [17]
9.9			EDXRD [37]
	8.7		X-ray and Mössbauer spectroscopy [14]
8.8	12.8	4.0	ADXRD [38]
9.3	11.7	2.4	ADXRD [39]

[a] XRD and EDXRD indicate X-ray diffraction and angular-dispersive X-ray diffraction, respectively.

given by various theoretical calculations [18–22]. For instance, the linear combination of Gaussian-type orbitals Hartree–Fock [18] predicted a B4-to-B1 phase transition at 8.57 GPa, whereas the full-potential linear muffin-tin orbital approach to density-functional theory within the local-density and generalized gradient approximation [22] and the atomistic calculations based on an inter-atomic pair potential within the shell-model approach [23] predicted the pressures for the same phase transition were 8.0 and 10.45 GPa, respectively. As a result, a reference point of 9.4 ± 0.7 GPa is taken as the B4-to-B1 phase transition pressure of bulk ZnO.

On the other hand, the path by which the B4-to-B1 phase transition takes place in bulk ZnO is still in debate. Saitta and Decremps [23] suggested that the B4 phase is converted to the B1 phase via a tetragonal path, whereas the hexagonal path model was considered to be preferable by Limpijumnong and Jungthawan [24]. The relative position of the oxygen and zinc sublattices along the c-axis (i.e., the internal structural parameter u) and the axial ratio (c/a, where c and a are cell parameters) are different in the two proposed models. For the hexagonal path, the values of parameters u and c/a first changes continuously from $u = 0.375$ and $c/a = 1.61$ to $u = 0.5$ and $c/a = 1.29$, respectively. Then the γ angle of the hexagon was increased from 60° to 90° during B4-to-B1 phase transition. For the tetragonal path, model has shown that the values of parameters c/a and γ first changes continuously from $c/a = 1.61$ and $\gamma = 60°$ to $c/a = 1.74$ and $\gamma = 90°$, respectively. Then the u parameter is increased from $u = 0.375$ to $u = 0.5$ during the B4-to-B1 phase transition. Moreover, each oxygen (zinc) atom also locates differently in the hexagonal and tetragonal path models. Namely, the oxygen (zinc) atom locates at the center of the equilateral triangle formed by three zinc (oxygen) atoms in the former model, while they are locating at the body center of the square pyramid formed by five zinc (oxygen) atoms in the latter case.

In addition to the results obtained from pure ZnO bulks, some important results of the pressure-induced phase transition for $Zn_{1-x}Mn_xO$ ternary compounds have also been reported. Wang et al. [25] used the energy-dispersive X-ray diffraction (EDXRD) method to demonstrate a significant change in the B4-to-B1 phase transition pressure in Mn-doped ZnO. Namely, the starting (completing) pressures of the B4-to-B1 phase transition were changed from 9.5 (11) GPa for pure ZnO to 8.3 (12) GPa for $Zn_{0.99}Mn_{0.01}O$ and 6.5 (9) GPa for $Zn_{0.98}Mn_{0.02}O$ crystals, respectively. The existence of manganese ions in the ZnO crystal appears to have substantially reduced the phase transition barrier, and hence lowered the pressure required to trigger the phase transition. However, the effect of manganese doping on the path of B4-to-B1 phase transition has remained largely unanswered. In this present study, the pressure-induced phase transition, compressibility, equation of state and phase transition path in $Zn_{0.98}Mn_{0.02}O$ were systematically investigated by angular dispersive X-ray diffraction (ADXRD) to explore this issue as well as to unveil the effect of the Mn-3d electrons on Zn–O bonding which might be important to the associated RTFM.

2. Experimental details

Specimens with the nominal composition of $Zn_{0.98}Mn_{0.02}O$ used in this study were prepared by conventional solid-state reaction method using MnO_2, $LiCO_3$, and ZnO with the purity better than 99.9% as the starting materials. The powders were mixed and ground with acetone in a zirconium oxide ball mill for 12 h. The mixed powders were then calcined in air at 1173 K for 5 h. To assure the homogeneous reaction of the starting powders, the grounding and calcined processes were repeated for 3 times. The stoichiometry of the Mn/Zn ratio in the obtained powders was checked using the energy dispersive X-ray spectroscopy attached in the scanning electron microscope (SEM, Hitachi S-4700).

ADXRD experiments were performed using a symmetric diamond anvil cell (DAC) with full X-ray aperture around 85° and the diffraction angle 2θ up to 38°. The X-ray energy was 16 keV and distance between sample and detector was 330 mm under high pressures [26]. The AISI301 stainless steel gasket material was pre-indented to 70–80 μm from an initial thickness of 250 μm. A 235 μm sample chambers were drilled in the center of the indented gaskets for the high pressure experiments using a discharge machine. Fine ruby powders were placed inside the hole as the pressure gauge and silicon oil was used as a pressure-transmitting medium [27]. The ground samples were placed on top of the ruby powders and the ruby fluorescence spectra were measured at the same spot. The pressures for high pressure ADXRD measurements within the DAC were determined by the shifts of fluorescence lines of ruby, using the calibration of Mao et al. [28].

ADXRD measurements were performed using the beamline BL01C2 [29] at the National Synchrotron Radiation Research Center (NSRRC), Taiwan, and beamline BL12B1 at SPring8, Japan. The wavelengths were 0.7749 Å (16 keV) and 0.7834 Å (15.825 keV) for BL01C2 and BL12B1, respectively. Diffraction patterns for $Zn_{0.98}Mn_{0.02}O$ samples were recorded up to a pressure of 13.80 GPa at a distance of 260 mm from the sample with a Mar 3450 image plate (IP) and a CCD online systems for BL01C2 and BL12B1, respectively. The sample-to-detector distance and spatial distortion of the IP and CCD detectors were corrected using diffraction patterns of CeO_2 powder. The observed intensity on the IP and CCD were integrated as a function of 2θ to obtain the one-dimensional diffraction profile using ESRF Fit2D code [30]. The unit cell parameters of the sample were obtained by using the program package GSAS (General Structure Analysis System) [31]. Final values of the lattice parameters were obtained using the Rietveld refinement, which refined user-selected parameters by minimizing the difference between an experimental pattern and a shape based on the composite crystal structure and instrumental parameters. Five parameters, namely the scale factor, background, lattice parameters, zero shift (specimen displacement), and thermal parameters are used to refine information in this work. Theoretically, n diffraction peaks, each peak serving as an observable, can refine $n-1$ parameters. Thus, the DAC with diffraction angle 2θ up to 38° at 16 keV can adequately match the required conditions of the Rietveld refinement.

3. Results and discussion

In situ ADXRD spectra of bulk $Zn_{0.98}Mn_{0.02}O$ obtained for a loading run up to 13.80 GPa and unloading run to ambient pressure are shown in Fig. 1. All diffraction peaks at the ambient pressure (0.1 MPa–0 GPa) shown in Fig. 1 can be assigned to the B4 phase of the hexagonal structured ZnO. Furthermore, as is evident from Fig. 1, ADXRD patterns show no trace of manganese or manganese oxide clusters formed in the present $Zn_{0.98}Mn_{0.02}O$, suggesting a homogeneous doping of manganese atoms within the ZnO lattice. The unit-cell parameters for $Zn_{0.98}Mn_{0.02}O$ at ambient pressure determined from Fig. 1 are $a = b = 3.2482(1)$ Å, $c = 5.2035(1)$ Å and $V/Z = 23.773(1)$ Å [3], respectively. These are slightly larger than the reported value of $a = b = 3.2465(8)$ Å, $c = 5.2030(19)$ Å and $V/Z = 23.745$ Å [3] (Inorganic Crystal Structure Database (ICSD)
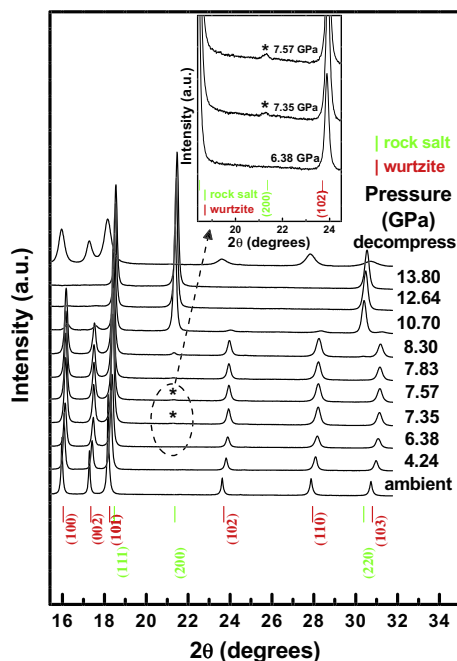
Fig. 1. Representative ADXRD patterns of bulk $Zn_{0.98}Mn_{0.02}O$ at elevated pressures and decompression. Bulk $Zn_{0.98}Mn_{0.02}O$ exhibited a phase transition with an onset pressure of 7.35 GPa marked with ∗ in the inset.

No. 94004) for hexagonal structured ZnO. Since the crystal ionic radius for Mn^{2+} (0.91 Å) is slightly larger than that of Zn^{2+} (0.83 Å) [7], the present observation, in fact, also suggests a homogeneous doping of manganese atoms and is consistent with the absence of impurity phases (see the Fig. 1).

The inset of Fig. 1 shows that, as the pressure reaches 7.35 GPa, a discernible new diffraction peak (marked with an asterisk) corresponding to the (2 0 0)-reflection of B1 phase starts to emerge for bulk $Zn_{0.98}Mn_{0.02}O$. Moreover, although the intensity of the new peak grows substantially with the increasing pressure, coexistence of diffraction peaks from the original B4 phase is evident over a wide range of pressures (7.35–12.46 GPa), indicating that the phase transition is taking place locally rather than globally. The starting and completing pressures of the B4-to-B1 phase transition observed in the present bulk $Zn_{0.98}Mn_{0.02}O$ are slightly larger and wider than that (6.5–9 GPa) reported by Wang et al. [25]. Based on the thermodynamics arguments that the transition pressure should be close or equal to the onset pressure, therefore, the transition pressure of B4 to B1 for bulk $Zn_{0.98}Mn_{0.02}O$ is taken as 7.35 GPa. Comparing to the starting pressures shown in Table 1 for the pure ZnO, our data also indicate that the manganese ion doping has resulted in a reduction of the transition pressure. Finally, the lattice parameters at 7.35 GPa for the present bulk $Zn_{0.98}Mn_{0.02}O$ are a = 3.2063(1) Å, c = 5.1318(2) Å and V/Z = 22.844(1) Å [3] for the B4 phase and, a = 4.2287(12) Å, V/Z = 18.905(16) Å [3] for the B1 phase, respectively; implying that the transition from B4 to B1 phase is accompanied by a substantial volume decrease of ~15.9%. As a result, when the pressure is released back to the ambient pressure tremendous amount of strain remained in the sample, albeit the bulk $Zn_{0.98}Mn_{0.02}O$ has essentially reverted to the B4 phase from the metastable B1 phase, as is evident from the drastic broadening of the corresponding diffraction peaks displayed in Fig. 1.

The volume vs. pressure data measured at the ambient temperature for bulk $Zn_{0.98}Mn_{0.02}O$ is shown in Fig. 2(a). The data for the B4 phase were fitted to the third-order Birch–Murnaghan equation of state [32]. The zero-pressure isothermal bulk moduli (B_0) and its

first derivative with respect to pressure (B_0') for B4 phase were fitted to be 157 ± 8 GPa and 8 ± 3, respectively. The pressure evolution of the reduced lattice parameters a/a_0, and c/c_0 of the B4 phase are presented in Fig. 2(b). Upon P = 7.35 GPa, the linear compressibility K_c = − $(1/c)(dc/dP)_T$ = 0.001576 GPa^{-1} along c-axis is larger than K_a = 0.001385 GPa^{-1}. The fact that the compression rate along the c-axis is higher indicates that the spacing between O and Zn(Mn) is more compressible than those between Zn(Mn) and Zn(Mn) ions. Consequently, the lattice is more susceptible to deform along the c axis under pressure. Fig. 2(c) shows the weight fraction (Wt. Frac.) as a function of pressure for both B4 and B1 phases. The results indicate that in the intermediate pressure range B4 and B1 phases coexist and the amount of increasing B1 corresponds well with that of the decreasing B4 as the pressure is continuously increased. This again indicates that the phase transition is taking place locally rather than globally. The pressure of equal weight fraction value (50:50) of B4 and B1 phases is around 9.5(1) GPa by a sigmoidal fit of Boltzmann function.

In Fig. 3, the internal structural parameter u and the c/a ratio obtained from the Rietveld refinements for bulk $Zn_{0.98}Mn_{0.02}O$ are plotted as a function of pressure. Our data indicate that the c/a ratio is ~1.602 for B4 phase at ambient pressure, which is slightly smaller than the reported values of 1.61 for pure ZnO [23,24] and deviates substantially from the value of 1.633 for the ideal c/a ratio of würtzite structure with a hexagonal unit cell, respectively. Kisi and Elcombe [33] pointed out that when the larger the difference between the electronegativity of the two constituents in hexagonal compounds the more deviation of the c/a ratio from the ideal value. The electronegativity using the Pauling scale [34] for Mn, Zn and O are 1.55, 1.65 and 3.44, respectively. The electronegativity difference between Mn and O is slightly larger than that between Zn and O. Therefore, the fact that the c/a ratio for bulk $Zn_{0.98}Mn_{0.02}O$ is smaller than that for pure ZnO is also in line with the conjecture that the doped manganese is randomly distributed within the ZnO lattice forming DMS. It is also evident from Fig. 3 that the c/a ratio decreases continuously from ~1.602 to ~1.597 as the pressure is increased from $P \cong 0$ GPa to $P \cong 12.6$ GPa, reflecting an obvious decreasing trend in the volume fraction of the B4 phase. The relationship between the c/a ratio and P can be fitted by a quadratic polynomial function with: $c/a = 1.6014 + 1.0879 \times 10^{-4}\ P - 3.1624 \times 10^{-5}\ P^2$. It is noted that, unlike that reported in Saitta and Decremps [23], our results do not show an abrupt drop in the c/a ratio to 1.29 amid the pressure-induced phase transition. On the other hand, in our case the u value decreases slightly from 0.384 to 0.371 as the pressure is increased from the ambient pressure to 6.38 GPa. Nevertheless, at $P \cong 7.35$ GPa, the u value undergoes a precipitous drop from 0.371 to 0.355 (i.e. ~4.3% change) and then increase rapidly to $u \approx 0.475$ at $P \approx 12.64$ GPa, beyond which the B4 phase converts to the B1 phase completely. Although it is not clear at present what causes the discontinuous drop in the u value, it apparently coincides with the onset pressure of the B4-to-B1 phase transition. Except for the anomaly at P = 7.35 GPa and despite of the relatively insensitive pressure dependence for P < 6.38 GPa, the trend still indicates that u value is in general increasing with increasing pressure. This observation is indicative that the B4-to-B1 phase transformation in bulk $Zn_{0.98}Mn_{0.02}O$ is more likely via the hexagonal rather than the tetragonal path [24].

Özgür et al. [35] reported that the u value can be alternatively described as the bond length or the nearest-neighbor distance between O and Zn(Mn) ions measured the c-axis (d_{nn-c}) divided by c. The bond length of equilateral triangle (d_{et}) and d_{nn-c} are plotted as a function of pressure, as shown in Fig. 4(a). It is seen that d_{nn-c} initially decreases slightly from ~2.000 Å at ambient pressure to ~1.909 Å at 6.38 GPa, then undergoes a discontinuous drop from 1.909 Å to 1.822 Å (~4.3%) at 7.35 GPa, and subsequently increases rapidly up to 2.424 Å at 12.64 GPa. On the other hand, d_{et} initially
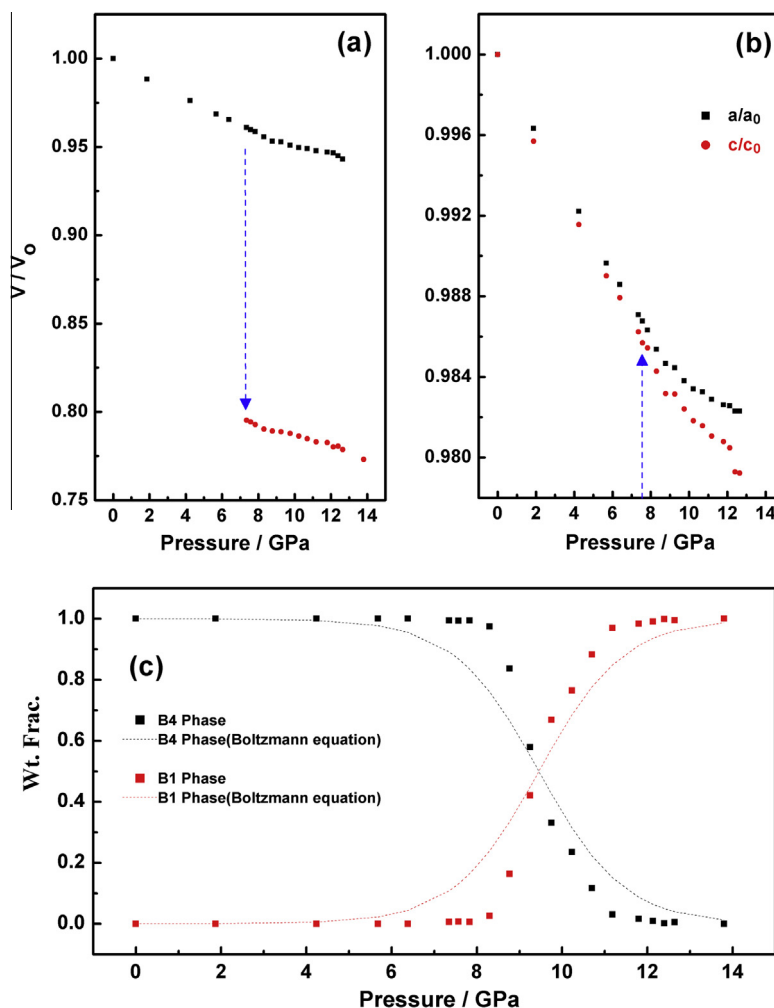
Fig. 2. (a) Pressure dependence of the V/V_0 of bulk $Zn_{0.98}Mn_{0.02}O$ at 300 K. (b) The change of bulk $Zn_{0.98}Mn_{0.02}O$ cell parameters a, and c with increasing pressures. (c) The weight fraction (Wt. Frac.) of B4 and B1 phases at 300 K in bulk $Zn_{0.98}Mn_{0.02}O$.
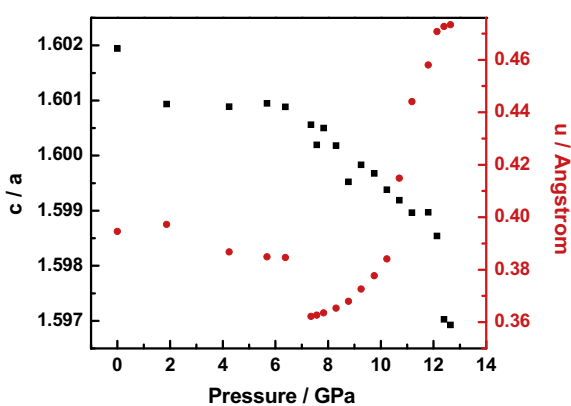
Fig. 3. Pressure dependence of c/a ratio (black solid squares) and the internal structural parameter u of würtzite structure $Zn_{0.98}Mn_{0.02}O$ (red solid circles) as a function of pressure obtained from Rietveld refinement. (For interpretation of the references to color in this figure legend, the reader is referred to the web version of this article.)

decreases slightly from 1.954 Å at ambient pressure to 1.947 Å at 6.38 GPa, then undergoes an abrupt rise from 1.947 Å to 1.982 Å (~1.8%) at 7.35 GPa, and immediately decreases rapidly down to 1.845 Å at 12.64 GPa. At $P \approx 7.35$ GPa, d_{nn-c} and u have a similar pressure dependence trend. Interestingly, as is evident from

Fig. 4(b), the pressure dependence of d_{et} exhibits an opposite trend to that of d_{nn-c} and u. Both of them display an abnormal turn at $P = 7.35$ GPa, which is also coincident with the onset pressure of the B4-to-B1 phase transition. The intimate relevance of the bond length anomalies and structural changes further affirm that the transition pressure of B4-to-B1 for bulk $Zn_{0.98}Mn_{0.02}O$ is indeed taking place at $P \approx 7.35$ GPa. The question remains to be addressed is the apparent lowering of the onset pressure of phase transition induced by Mn-doping.

To explain the reduction of the phase-transition pressure of bulk $Zn_{0.98}Mn_{0.02}O$, it is heuristic to compare the behaviors observed in DMS's with similar crystal structures. Maheswaranathan et al. [36] reported that, in cadmium telluride (CdTe), substituting zinc with cadmium in the zinc-blende lattice evidently led to more stable lattice in $Cd_{0.52}Zn_{0.48}Te$ than with manganese in $Cd_{1-x}Mn_xTe$ with $0 \leqslant x \leqslant 0.52$. They also disclosed that manganese was responsible for making the zinc-blende crystal structure more susceptible to the applied pressure instead of zinc. In that the relatively loosely bounded $3d$ electrons in manganese are preferably hybridized into the tetragonal bonds. On the contrary, the cadmium and zinc d levels do not hybridize with the sp^3 bonding orbitals. Consequently, it was concluded that the cause of the reduction of the phase transition pressure observed in the manganese ternary alloys was induced mainly by the hybridization of the manganese or iron $3d$ orbitals into the tetrahedral bonds. Fig. 4(b) shows schematically that the hybridization of manganese $3d$ orbitals into the
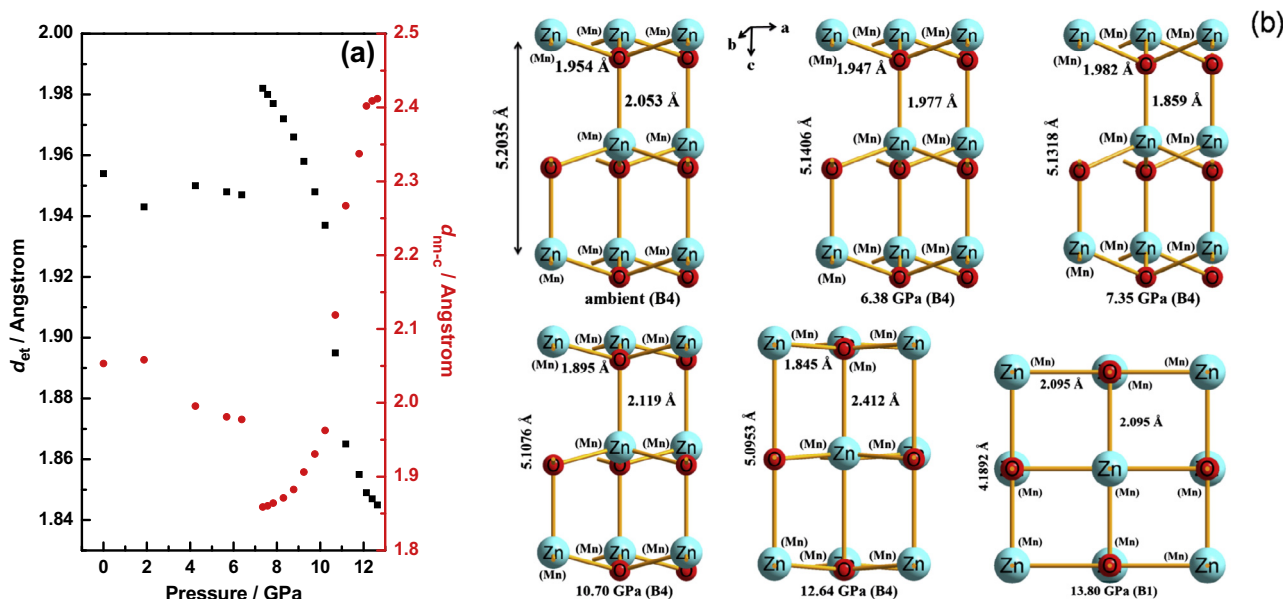
Fig. 4. The pressure dependence of (a) the bond length of equilateral triangle (d_{et}) and the nearest-neighbor distance of O to Zn(Mn) parallel to the c axis (d_{nn-c}) and (b) the anomalous pressure dependence of the increased trend of the nearest-neighbor distance of O to Zn(Mn) parallel to the c axis and decreased trend of the bond length of equilateral triangle.

tetrahedral bonds would weaken the würtzite phase structure, which not only reduces the phase transition pressure but also forces the d_{nn-c} to increase and d_{et} to decrease to bring Zn(Mn) to rocksalt structure. In our case here, it appears that the loosely bounded manganese 3d electrons of may have effectively stretched d_{nn-c} and brought Zn(Mn) to rocksalt structure, which in turn reduces the stability of B4 phase of bulk $Zn_{0.98}Mn_{0.02}O$ under the application of pressure.

4. Conclusion

In summary, high pressure ADXRD studies on bulk $Zn_{0.98}Mn_{0.02}O$ up to 13.80 GPa were systematically performed. The results reveal that the B4-to-B1 phase transition in this Mn-doped diluted magnetic semiconductor has an onset pressure of ~7.35 GPa. The compressibility of bulk $Zn_{0.98}Mn_{0.02}O$ is anisotropic with that along c-axis being larger than along a-axis. The largest change in the u value with increasing pressure appears to result from the stretching of the nearest-neighbor distance of O to Zn(Mn) parallel to the c axis for bulk $Zn_{0.98}Mn_{0.02}O$. Under high pressure, the effect of the manganese 3d electrons on increasing the nearest-neighbor distance of O to Zn(Mn) parallel to the c axis may have played the primary role dictating the phase transition of bulk $Zn_{0.98}Mn_{0.02}O$. The bond weakening results in a structural distortion prior to phase transition under high pressure as revealed by the anomalous pressure dependence of the increased trend of the nearest-neighbor distance of O to Zn(Mn) parallel to the c axis under the application of pressure. The fitting with equation of state for the bulk $Zn_{0.98}Mn_{0.02}O$ gave a bulk modulus of 157(8) GPa and a value of 8(3) for its first derivative. Detailed analyses on the pressure-dependent u value indicate that the B4-to-B1 phase transformation in bulk $Zn_{0.98}Mn_{0.02}O$ is more likely via the hexagonal rather than the tetragonal path. More theoretical work is needed to explore the possible structure for the high-pressure phase of bulk $Zn_{0.98}Mn_{0.02}O$.

Acknowledgements

References

[1] A. Ohtomo, K. Tamura, M. Kawasaki, T. Makino, Y. Segawa, Z.K. Tang, G.K.L. Wong, Y. Matsumoto, H. Koinuma, Appl. Phys. Lett. 77 (2000) 2204.
[2] F.H. Leiter, H.R. Alves, A. Hofstaetter, D.M. Hoffmann, B.K. Meyer, Phys. Status Solidi B 226 (2001) R4.
[3] F.H. Leiter, H.R. Alves, N.G. Romanov, D.M. Hoffmann, B.K. Meyer, Physica B 340–342 (2003) 201.
[4] H. Saeki, H. Tabata, T. Kawai, Solid State Commun. 120 (2001) 439.
[5] K. Ueda, H. Tabata, T. Kawai, Appl. Phys. Lett. 79 (2001) 988.
[6] P. Sharma, A. Gupta, K.V. Rao, F.J. Owens, R. Sharma, R. Ahuja, J.M.O. Guillen, B. Johansson, G.A. Gehring, Nat. Mater. 2 (2003) 673.
[7] J. Luo, J.K. Liang, Q.L. Liu, F.S. Liu, Y. Zhang, B.J. Sun, G.H. Rao, J. Appl. Phys. 97 (2005) 086106.
[8] W. Chen, L.F. Zhao, Y.Q. Wang, J.H. Miao, S. Liu, Z.C. Xia, S.L. Yuan, Solid State Commun. 134 (2005) 827.
[9] J.H. Yang, L.Y. Zhao, Y.J. Zhang, Y.X. Wang, H.L. Liu, M.B. Wei, Solid State Commun. 143 (2007) 566.
[10] J. Das, D.K. Mishra, D.R. Sahu, S.K. Pradhan, B.K. Roul, J. Magn. Magn. Mater. 323 (2011) 641.
[11] A. Ramachandran, P. Kalaivanan, K. Gnanasekar, Superlattices Microstruct. 52 (2012) 1020.
[12] C.H. Bates, W.B. White, R. Roy, Science 137 (1962) 993.
[13] S.C. Yu, I.L. Spain, E.F. Skelton, Solid State Commun. 25 (1978) 49.
[14] H. Karzel, W. Potzel, M. Köfferlein, W. Schiessel, M. Sreiner, U. Hiller, G.M. Kalvius, D.W. Mitchell, T.P. Das, P. Blaha, K. Schwarz, M.P. Pasternak, Phys. Rev. B 53 (1996) 11425.
[15] J.C. Jamieson, Phys. Earth Planet. Inter. 3 (1970) 201.
[16] L. Gerward, J. Staun Olsen, J. Synchrotron Radiat. 2 (1995) 233.
[17] S. Desgreniers, Phys. Rev. B 58 (1998) 14102.
[18] J.M. Recio, M.A. Blanco, V. Luana, R. Pandey, L. Gerward, J.S. Olsen, Phys. Rev. B 58 (1998) 8949.
[19] J.E. Jaffe, A.C. Hess, Phys. Rev. B 48 (1993) 7903.
[20] J.E. Jaffe, J.A. Snyder, Z. Lin, A.C. Hess, Phys. Rev. B 62 (2000) 1660.
[21] R. Ahuja, L. Fast, O. Eriksson, J.M. Wills, B. Johansson, J. Appl. Phys. 83 (1998) 8065.
[22] A. Zaoui, W. Sekkal, Phys. Rev. B 66 (2002) 174106.
[23] A.M. Saitta, F. Decremps, Phys. Rev. B 70 (2004) 035214.
[24] S. Limpijumnong, S. Jungthawan, Phys. Rev. B 70 (2004) 054104.
[25] Y. Wang, Y. Zhang, W.J. Chang, G.L. Lu, J.Z. Jiang, Y.C. Li, J. Liu, T.D. Hu, J. Phys. Chem. Solids 66 (2005) 1775.
[26] Y.C. Kao, T. Huang, D.Y. Lin, Y.S. Huang, K.K. Tiong, H.Y. Lee, J.M. Lin, H.S. Sheu, C.M. Lin, J. Chem. Phys. 137 (2012) 024509.
[27] Y. Shen, R.S. Kumar, M. Pravica, M.F. Nicol, Rev. Sci. Instrum. 75 (2004) 4450.
[28] H.K. Mao, J. Xu, P.M. Bell, J. Geophys. Res. – Solid Earth Planets 91 (1986) 4673.

[29] Y.F. Song, C.H. Chang, C.Y. Liu, S.H. Chang, U.S. Jeng, Y.H. Lai, D.G. Liu, S.C. Chung, K.L. Tsang, G.C. Yin, J.F. Lee, H.S. Sheu, M.T. Tang, Y.K. Hwu, K.S. Liang, J. Synchrotron Radiat. 14 (2007) 320.
[30] A.P. Hammersley, S.O. Svensson, M. Hanfland, A.N. Fitch, D. Hausermann, High Pressure Res. 14 (1996) 235.
[31] A.C. Larson, R.B. Von Dreele, General Structure Analysis System (GSAS), Los Alamos National Laboratory Report LAUR 86-748, 2000.
[32] R.J. Hemley, Ultrahigh-Pressure Mineralogy: Physics and Chemistry of the Earth's Deep Interior, Mineralogical Society of America, Washington, DC, 1998.
[33] E. Kisi, M.M. Elcombe, Acta Crystallogr. C 45 (1989) 1867.

[34] L. Pauling, J. Am. Chem. Soc. 54 (1932) 3570.
[35] Ü. Özgür, Ya.I. Alivov, C. Liu, A. Teke, M.A. Reshchikov, S. Doğan, V. Avrutin, S.-J. Cho, H. Morkoç, J. Appl. Phys. 98 (2005) 041301.
[36] P. Maheswaranathan, R.J. Sladek, U. Debska, Phys. Rev. B 31 (1985) 5212.
[37] J.Z. Jiang, J.S. Olsen, L. Gerward, D. Frost, D. Rubie, J. Peyronneau, Europhys. Lett. 50 (2000) 48.
[38] H.Z. Liu, Y. Ding, M. Somayazulu, J. Qian, J. Shu, D. Hausermann, H.K. Mao, Phys. Rev. B 71 (2005) 4.
[39] L. Wang, H. Liu, J. Qian, W. Yang, Y. Zhao, J. Phys. Chem. C 116 (2012) 2074.